

1. Introduction

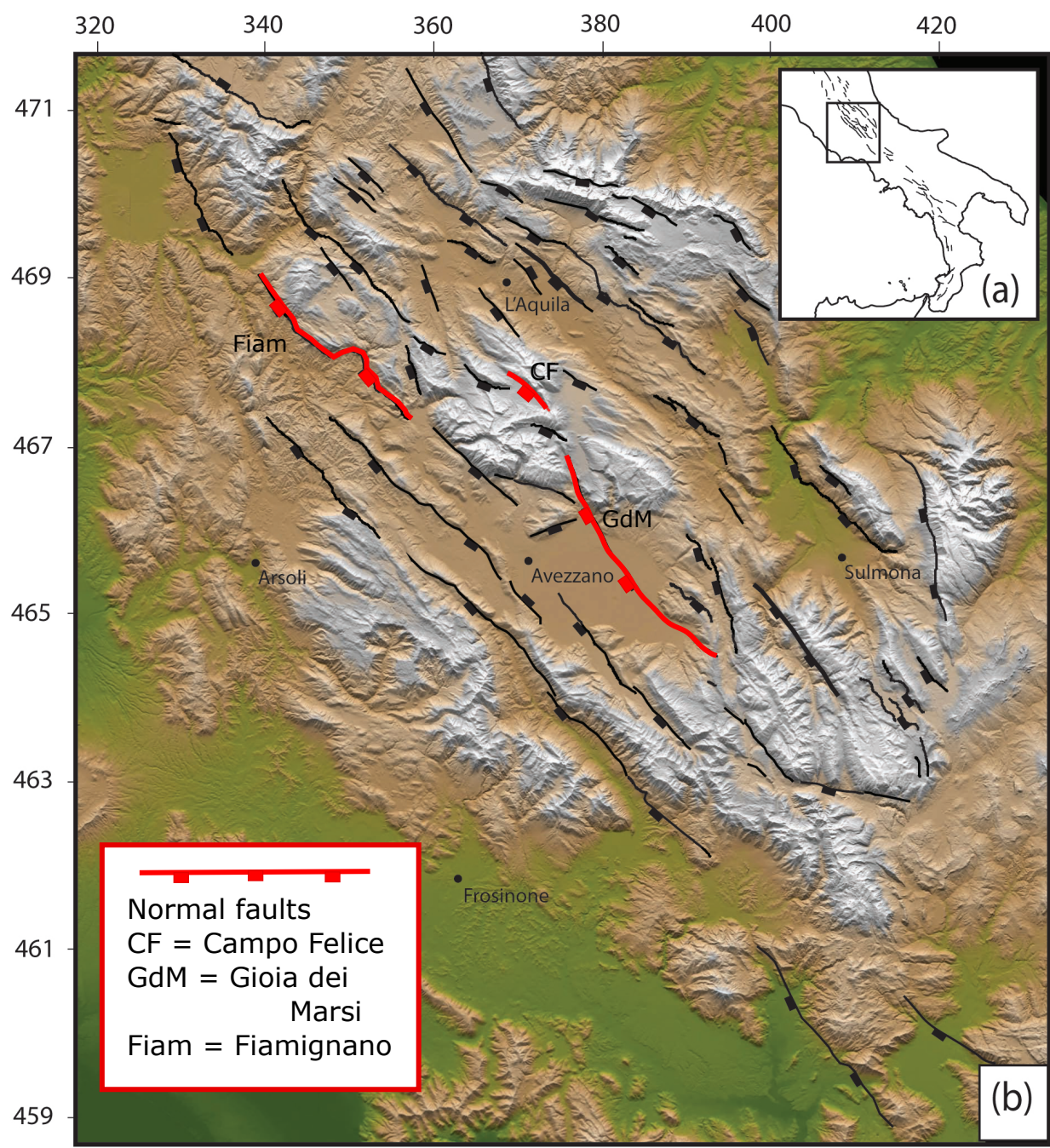


Figure 1a, location of primary study area, Abruzzo region, Central Italy, 1b area of normal faulting, adapted from Figure 2, Wilkinson et al 2015

"Squirreliness" is an "unofficial" term used in the UCERF (Uniform California Earthquake Rupture Forecast 3), denoting TAAD, or Total Absolute Angular Deviation, a measurement of the extent to which the surface trace of a fault rupture deviates internally from the overall strike of the fault. Biasi and Wesnousky (2017) used TAAD to analyse large scale fault traces (>5km), without accounting for topographical variations, quantifying the extent of internal bends along the fault (Figure 2) to derive a "squirrel" factor (expressed in degrees), plotted v. (a) length and (b) average curvature/km.

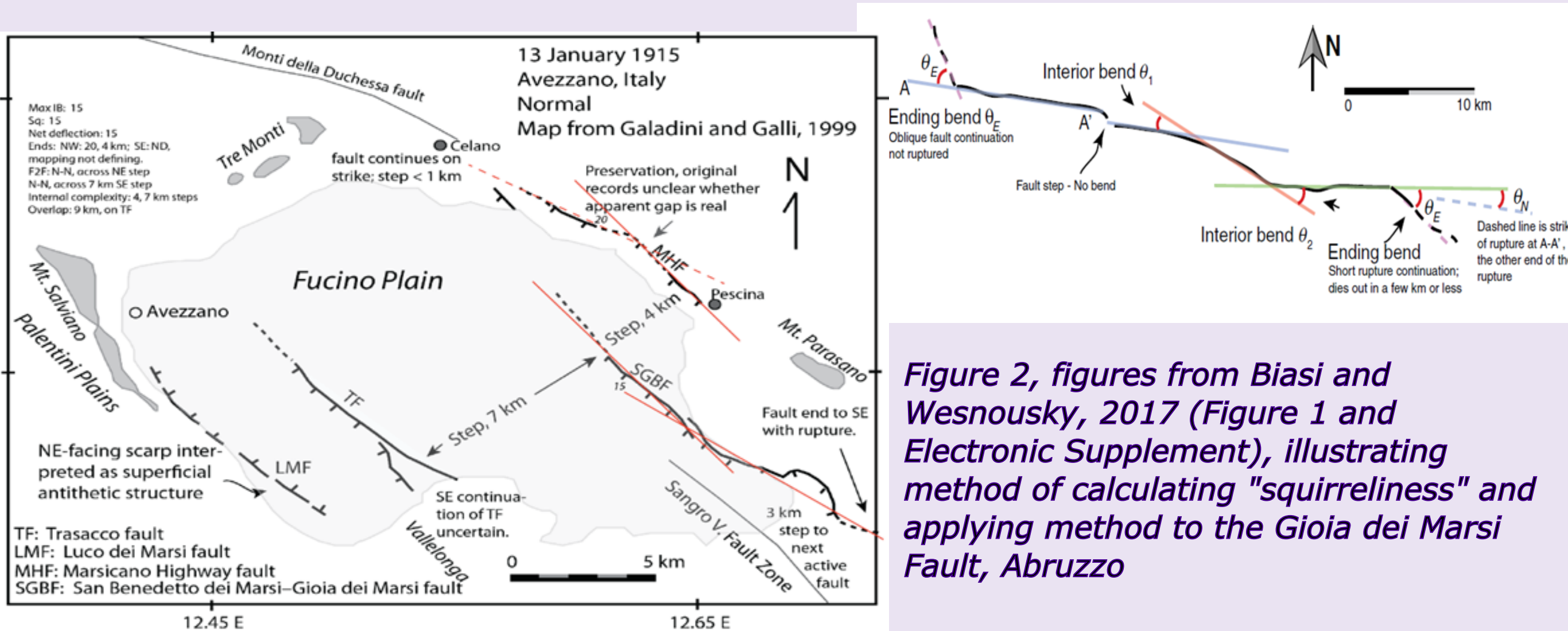


Figure 2, figures from Biasi and Wesnousky, 2017 (Figure 1 and Electronic Supplement), illustrating method of calculating "squirreliness" and applying method to the Gioia dei Marsi Fault, Abruzzo

This project adapts and develops this line of research, concentrating initially upon fault traces from active normal faults from the Apennine region, central Italy, including the Gioia dei Marsi, Campo Felice and Fiamignano Faults (Figures 3-5, locations marked in Figure 1). Many of those faults exhibit apparent sinuosity on the surface which is difficult to explain solely from local topographical features. The aim is to investigate relationships at a variety of scales, all smaller than the scale of Biasi and Wesnousky's research.



Figure 3 Gioia dei Marsi Fault (~1km)



Figure 4,Campo Felice Fault (~300m)

2. Methodology

The Apennine area, central Italy is thought to be well-suited to this method of analysis, given known or calculated strain rates since last Glacial Maximum ~15,000 years ago, field data including slip azimuth and plunge, and well established fault traces that have yielded length data from ~30 active normal faults within the Abruzzo region.

Quantifying surface rupture morphology of active normal faults

Bob Elliott, Ken McCaffrey, and Jonny Imber,
all Durham University

Department of Earth Sciences,
Durham University,
Science Labs,
Durham DH1 3LE
r.g.elliott@durham.ac.uk

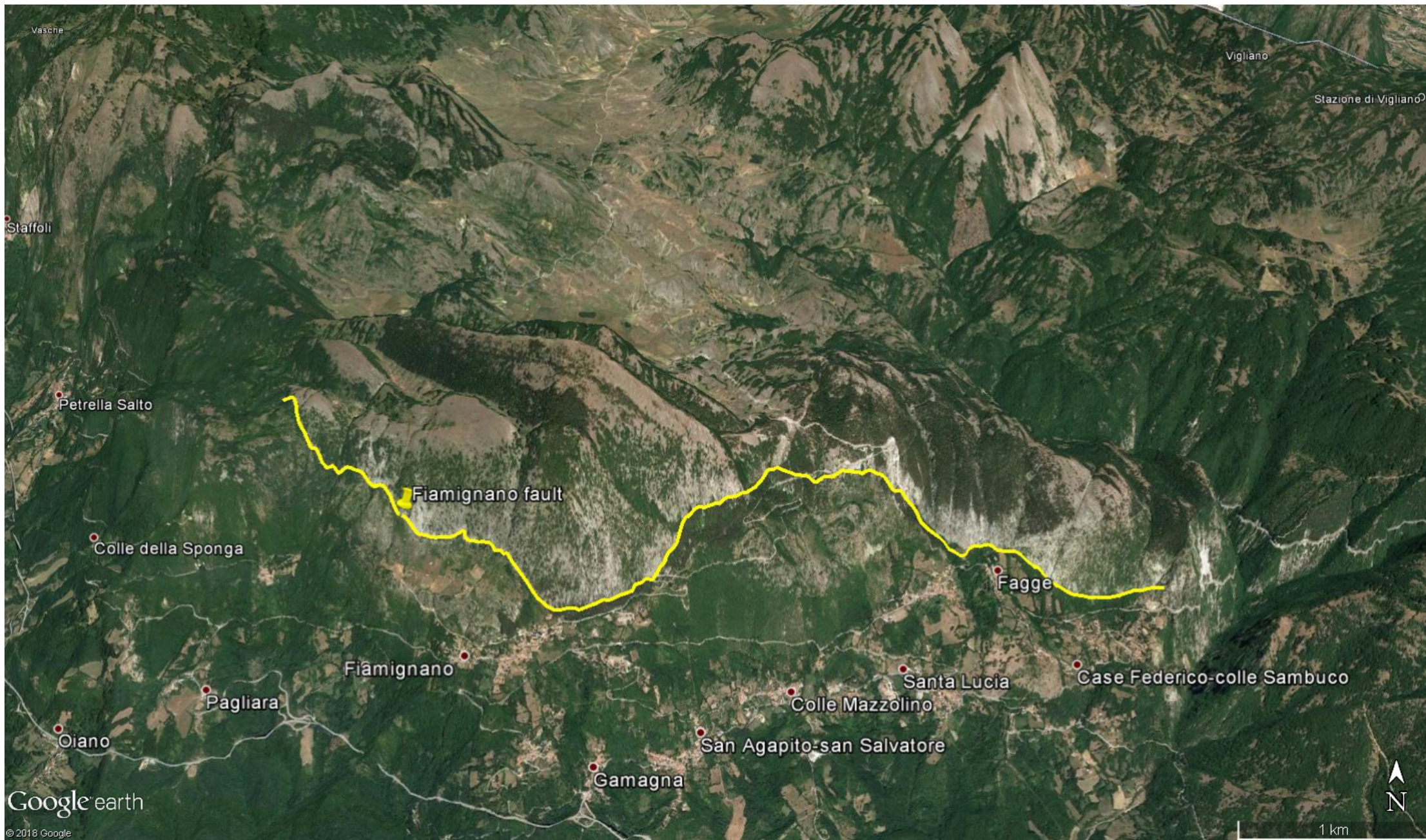


Figure 5, Fiamignano Fault, trace from Google Earth (SRTM) imagery, resolution 30m, trace is ~8 km in length

The datasets used are (1) Google Earth images (at 30m resolution) for all ~30 faults and (2) a mixture of aerial- and ground-based LiDAR images from 5 faults (covering ~2-4 km of each of those faults). In each case the fault traces are picked from the data (an example, the Fiamignano Fault, is at Figure 5). The SRTM fault traces are mapped at their fullest identifiable extent, and the LiDAR fault traces at a variety of scales (down to ~50 m segments). In each case:

- (1) The traces are exported as .shp files with 3D data to MOVE;
- (2) a plane is created from known slip azimuth and dip data;
- (3) a further plane is created orthogonal to that plane;
- (4) the trace is projected onto the latter plane (Figure 6);
- (5) the projected trace is measured for its "straight line" length (using the measuring tool in MOVE);
- (6) sinuosity is quantified by finding the ratio of projected length to straight line length (Figure 7).

Figure 6 screen shot from MOVE software showing creation of plane representing known slip surface for the Fiamignano Fault (225/42)SW from SRTM data (blue), orthogonal planar surface (purple), "picked" fault trace (yellow) and projected trace (red), North is looking into figure.

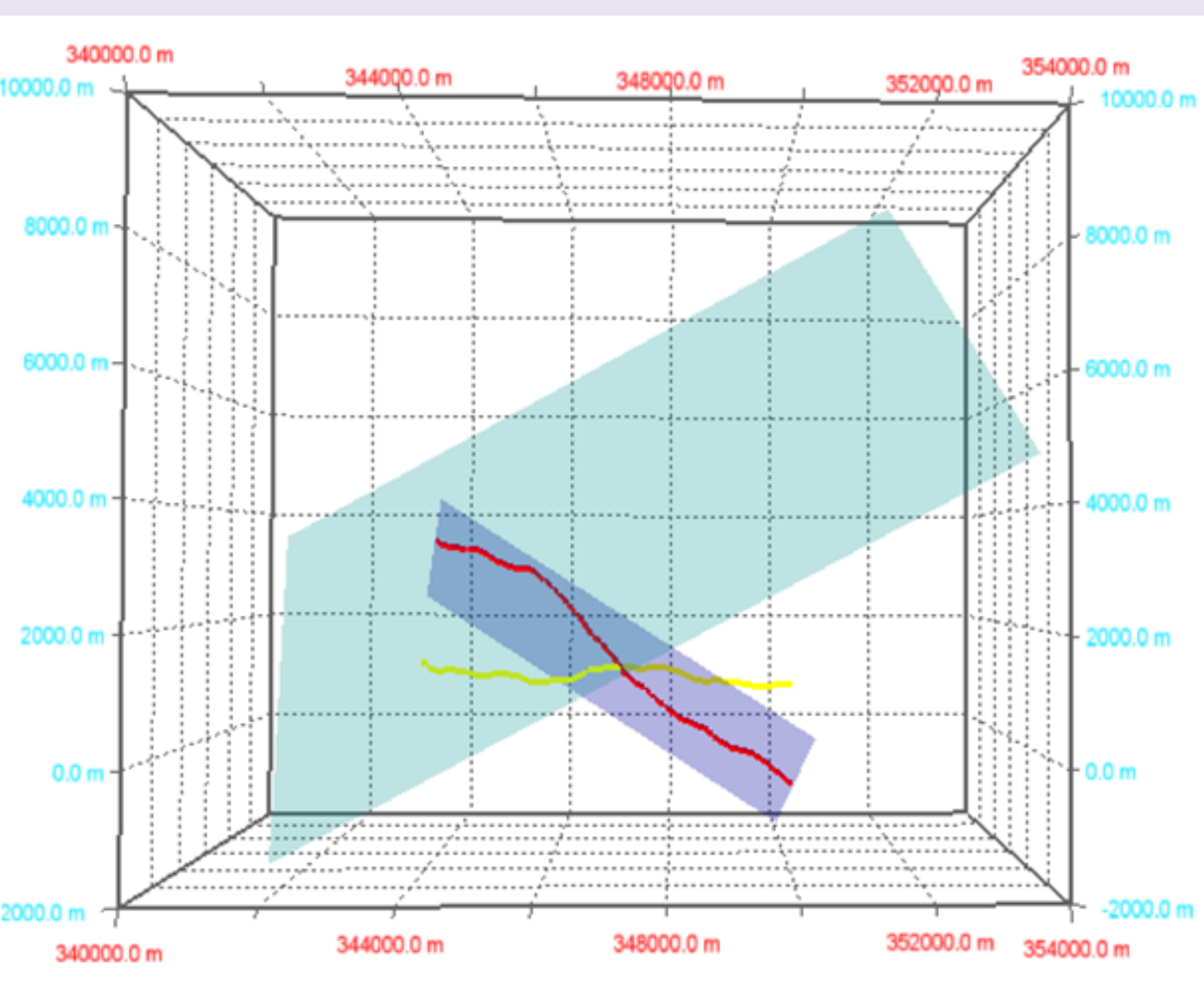
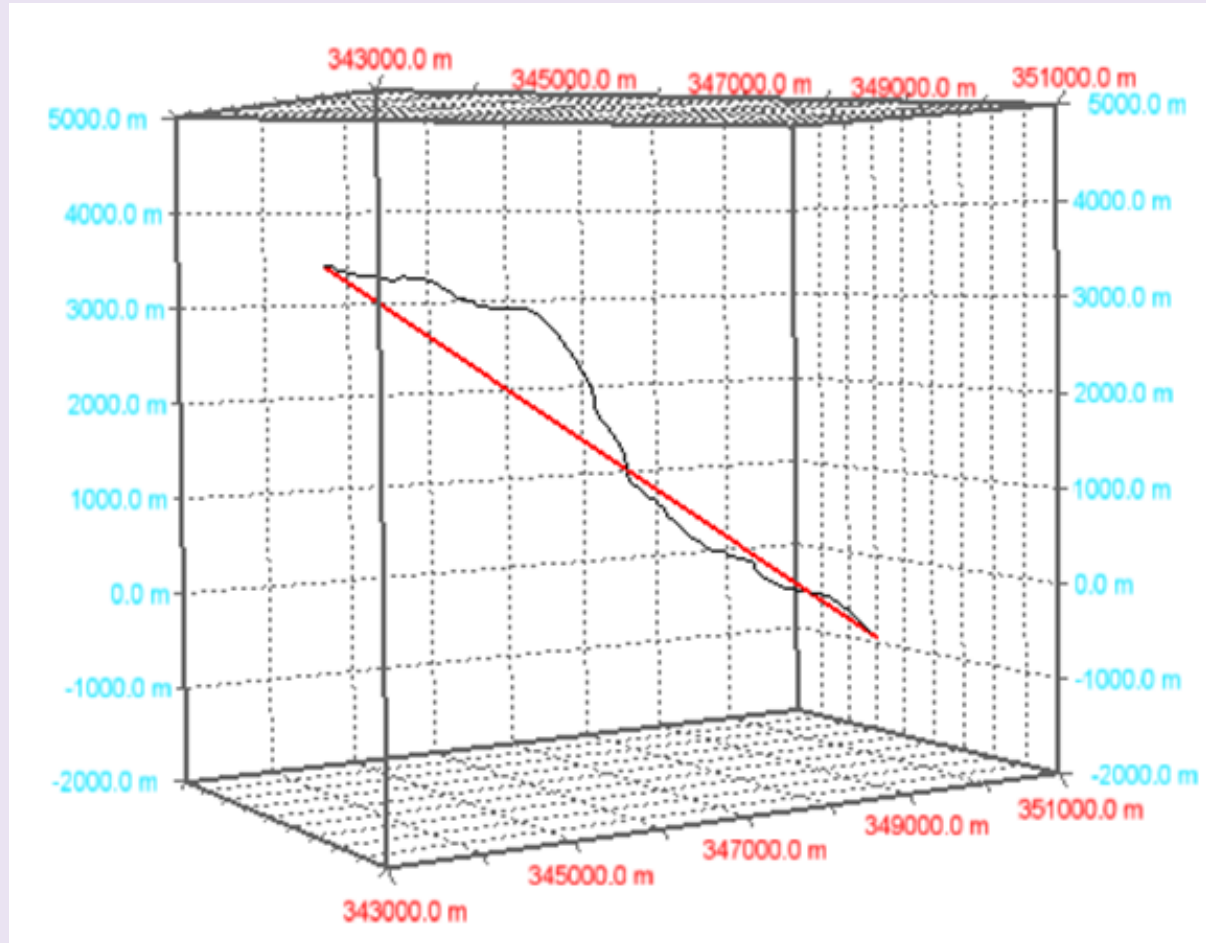


Figure 7, screen shot from MOVE showing comparison of straight line distance (red) to projected trace line (black) to calculate ratio for sinuosity (projected line/straight line distance)

The sinuosity values are plotted against a number of known variables, including fault length, projected trace length, and throw rate. The longer traces from the SRTM data (>5 km of mapped traces, representing >50% of the recorded fault length) are analysed to assess whether the figures for sinuosity vary depending upon whether the traces are within 1 km of the end of the recorded fault length. The shorter LiDAR data-derived traces are plotted along fault length to assess the variability of sinuosity along strike.

3. Results

Typical sinuosity figures are ~1.1 -1.2. Fiamignano's sinuosity figure is 1.148 from the SRTM images (mapped trace of ~7.8 km), and at a smaller scale (from airborne LiDAR) an average sinuosity of 1.205 (total mapped traces of ~1km). This is within the top 10% of sinuosity figures. The most sinuous is Velino-Magnola (weighted average sinuosity of 1.212, SRTM images). There may be some possible correlation between higher sinuosity figures and overall strikes of the faults which deviate from the regional trend. Other relationships are more difficult to assess; for example, there is a small degree of positive correlation between increasing throw rate and sinuosity (Figure 8), and a small degree of negative correlation between increasing trace length and sinuosity (longer traces) (Figure 9). However, neither is particularly significant statistically. Nor is there any clear distinction between "end" and "middle" traces from the longer faults mapped.

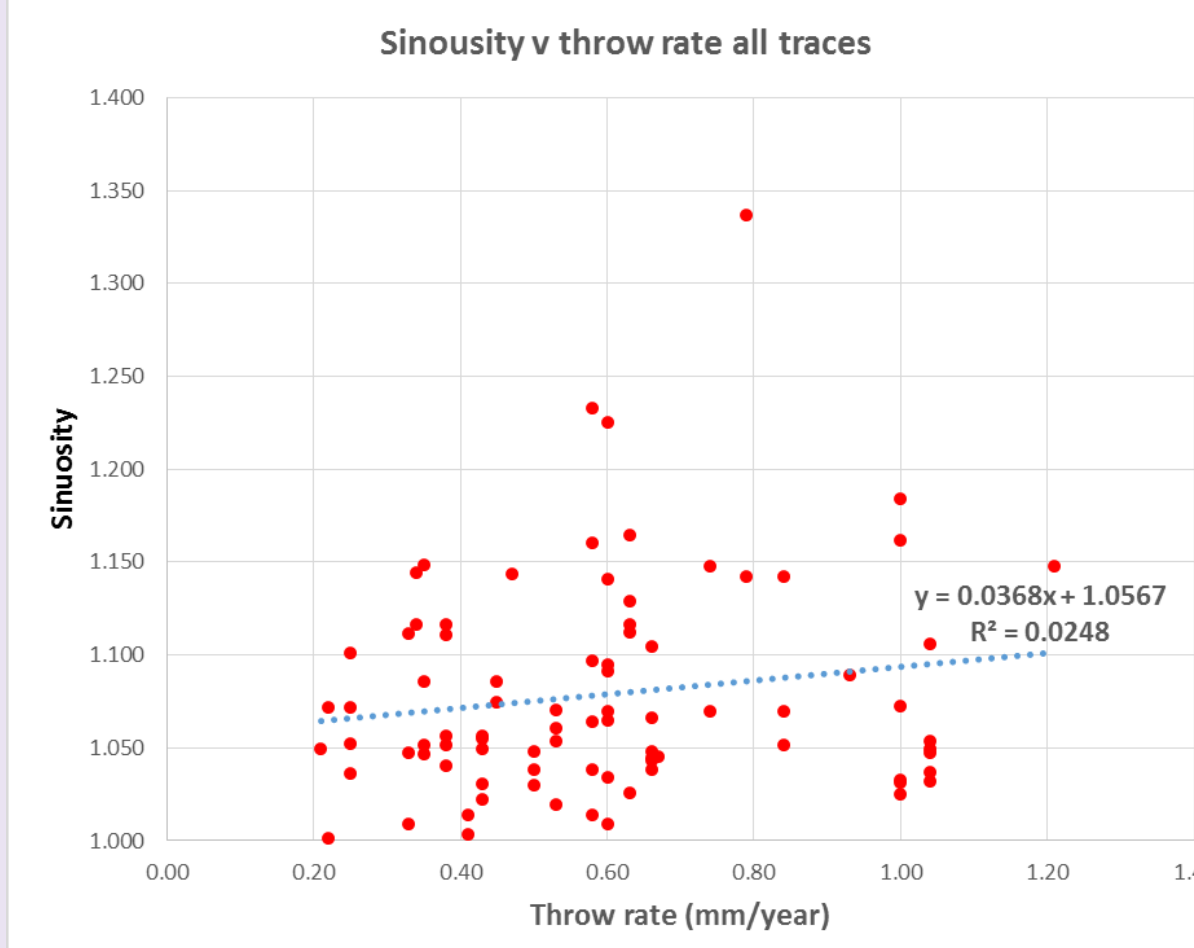


Figure 8, trace sinuosity values by throw rate (from SRTM data)

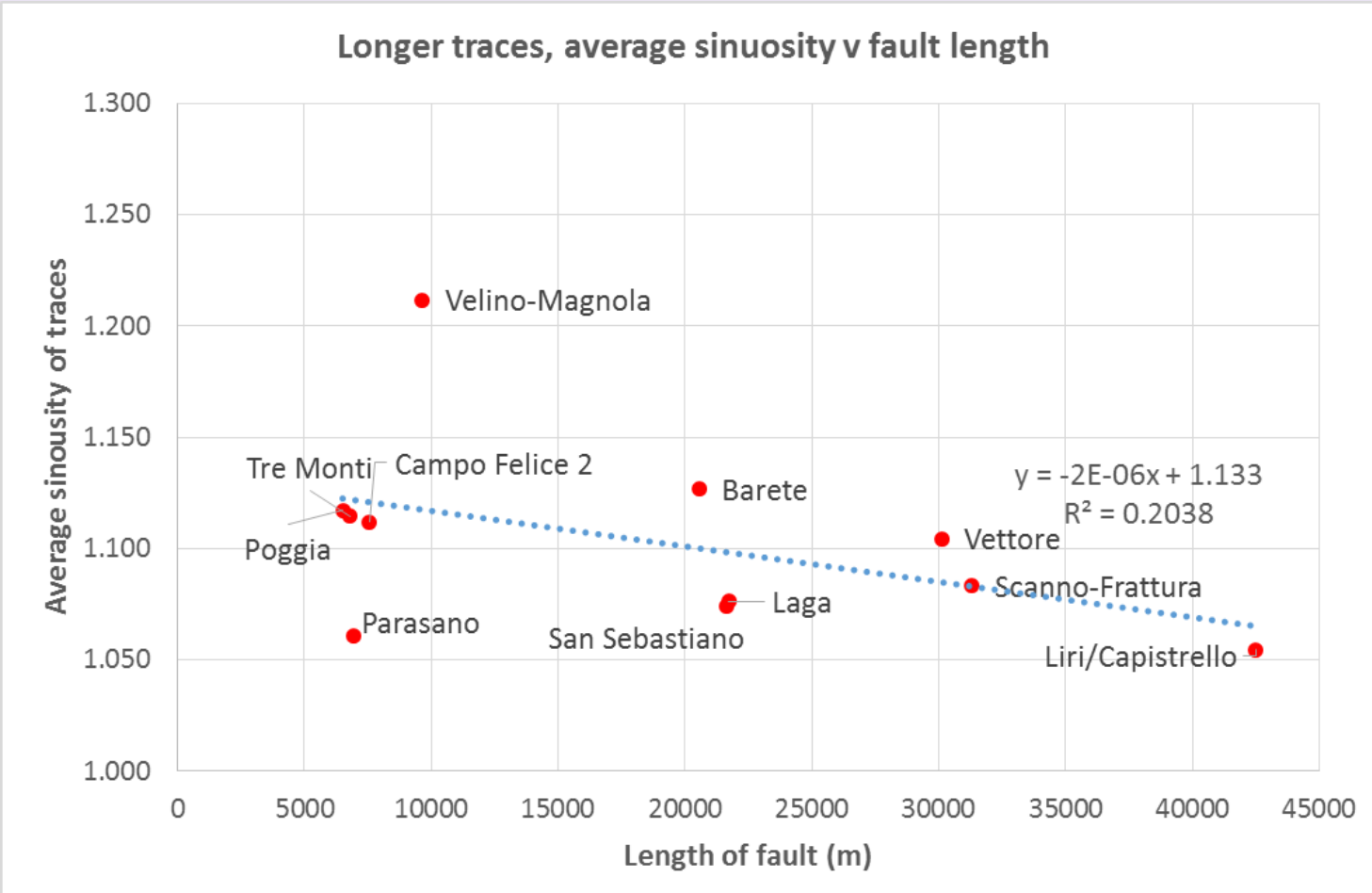


Figure 9, sinuosity values by fault length, longer traces (SRTM data)

More detailed work on the LiDAR data-derived traces is ongoing. A profile along strike for Fiamignano, using individual segments of ~80m shows little clear pattern (Figure 10), although distorted by a large bend seen at segment 12. Profiles from Parasano and Campo Felice show a general tendency towards greater sinuosity in the middle sections of the traces mapped.

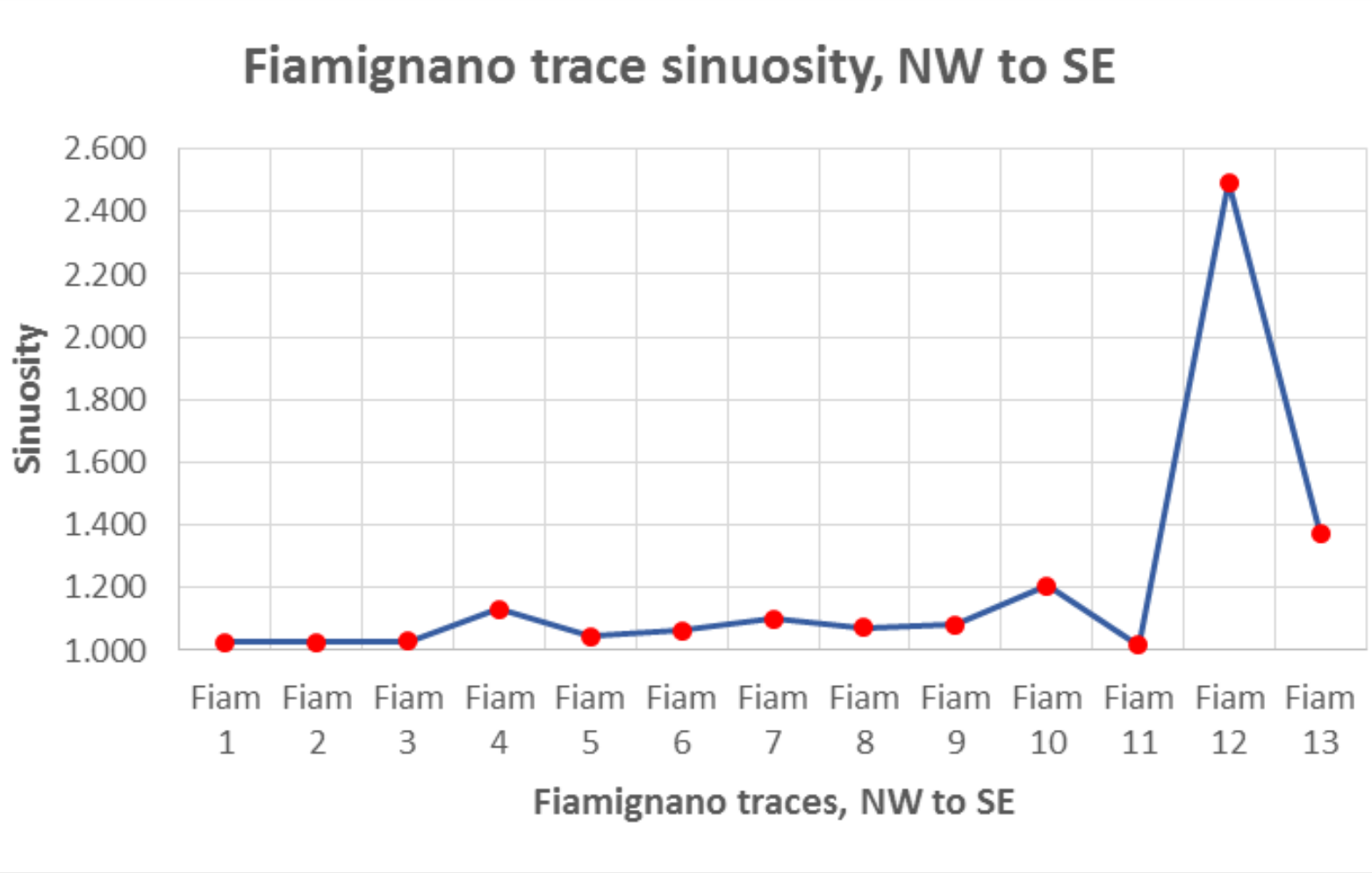


Figure 10, sinuosity profile along fault length for Fiamignano Fault, from NW to SE, using ~80m segments taken from LiDAR data.

4. Discussion and further work

The relationships noted so far are neither clear nor statistically compelling. Work is ongoing to establish the relationships more clearly. An initial aim will be to analyse the traces in smaller segments, and to construct more detailed along-fault strike profiles, enabling a more detailed study of local factors influencing sinuosity, such as fracture patterns. Available LiDAR datasets will enable this approach to be compared across 4-5 faults. The aim is to repeat the methodology in at least one other research area, probably including the Owens Valley volcanics, in California. The Apennine region is a relatively young fault network, predominantly involving carbonates. Investigating different lithologies with different histories of fault network growth is expected to lead to useful comparisons between the regions and lithologies, explaining any differences by reference to the geologies of the regions in question. Those observations may in turn help to provide insight into the proposed models of fault growth.

References

(1) Biasi, G.P., and Wesnousky, S.G., (2017), Bends and Ends of Surface Ruptures, Bulletin of the Seismological Society of America (2017) Vol 107(6), pp 2543-2560
(2) Bubeck, A., Wilkinson, M., Roberts, G.P., Cowie, P.A., McCaffrey, K.J.W., Phillips, R., Sammonds, P., 2015, The tectonic geomorphology of bedrock scarps of active normal faults in the Italian Apennines mapped using combined ground penetrating radar and terrestrial laser scanning, Geomorphology237 (2015) 38-51
(3) Jackson, C.A.-L., Bell, R.E., Rotevatn, A., Tvedt, A.B.M., 2017, Techniques to determine the kinematics of synsedimentary normal faults and implications for fault growth models, In Childs et al (2017) The Geometry and Growth of Normal Faults, Geological Society of London Special Publications vol 439(1), p187
(4) Wilkinson, M., Roberts, G.P., McCaffrey, K., Cowie, P.A., Faure Walker, J.P., Papanikolaou, I., Phillips, R.J., Michetti, A., Vittori, E., (2015), Slip distributions on active normal faults measured from LiDAR and field mapping of geomorphic offsets: an example from L'Aquila, Italy, and implications for modelling seismic moment release, Geomorphology, 2015, Vol 237, pp130-141
Figures 7 & 8 created with MOVE 2017.1 software (Midland Valley), fault traces from LiDAR created using Cloud Compare, Google Earth Images (c) Google Inc., Image Landsat/Copernicus, Data SIO, NOAA, US Navy, NGA, GEBCO